NASA/TM—2008-214998 07ATC–214

A Step Towards CO_2-Neutral Aviaton

Andreja Brankovic and Robert C. Ryder
Flow Parametrics, LLC, Ivoryton, Connecticut

Robert C. Hendricks
Glenn Research Center, Cleveland, Ohio

Marcia L. Huber
National Institute of Standards and Technology, Boulder, Colorado

August 2008

NASA STI Program . . . in Profile

Since its founding, NASA has been dedicated to the advancement of aeronautics and space science. The NASA Scientific and Technical Information (STI) program plays a key part in helping NASA maintain this important role.

The NASA STI Program operates under the auspices of the Agency Chief Information Officer. It collects, organizes, provides for archiving, and disseminates NASA's STI. The NASA STI program provides access to the NASA Aeronautics and Space Database and its public interface, the NASA Technical Reports Server, thus providing one of the largest collections of aeronautical and space science STI in the world. Results are published in both non-NASA channels and by NASA in the NASA STI Report Series, which includes the following report types:

- TECHNICAL PUBLICATION. Reports of completed research or a major significant phase of research that present the results of NASA programs and include extensive data or theoretical analysis. Includes compilations of significant scientific and technical data and information deemed to be of continuing reference value. NASA counterpart of peer-reviewed formal professional papers but has less stringent limitations on manuscript length and extent of graphic presentations.

- TECHNICAL MEMORANDUM. Scientific and technical findings that are preliminary or of specialized interest, e.g., quick release reports, working papers, and bibliographies that contain minimal annotation. Does not contain extensive analysis.

- CONTRACTOR REPORT. Scientific and technical findings by NASA-sponsored contractors and grantees.

- CONFERENCE PUBLICATION. Collected papers from scientific and technical conferences, symposia, seminars, or other meetings sponsored or cosponsored by NASA.

- SPECIAL PUBLICATION. Scientific, technical, or historical information from NASA programs, projects, and missions, often concerned with subjects having substantial public interest.

- TECHNICAL TRANSLATION. English-language translations of foreign scientific and technical material pertinent to NASA's mission.

Specialized services also include creating custom thesauri, building customized databases, organizing and publishing research results.

For more information about the NASA STI program, see the following:

- Access the NASA STI program home page at *http://www.sti.nasa.gov*

- E-mail your question via the Internet to *help@sti.nasa.gov*

- Fax your question to the NASA STI Help Desk at 301–621–0134

- Telephone the NASA STI Help Desk at 301–621–0390

- Write to:
  NASA Center for AeroSpace Information (CASI)
  7115 Standard Drive
  Hanover, MD 21076–1320

NASA/TM—2008-214998 07ATC–214

A Step Towards CO_2-Neutral Aviaton

Andreja Brankovic and Robert C. Ryder
Flow Parametrics, LLC, Ivoryton, Connecticut

Robert C. Hendricks
Glenn Research Center, Cleveland, Ohio

Marcia L. Huber
National Institute of Standards and Technology, Boulder, Colorado

Prepared for the
2007 Aerotech Congress and Exhibition
sponsored by the SAE International
Los Angeles, California, September 17–20, 2007

National Aeronautics and
Space Administration

Glenn Research Center
Cleveland, Ohio 44135

August 2008

Acknowledgments

The authors would like to thank Jih-Fen Lei and Gary Seng of the NASA Glenn Research Center as well as the National Institute of Standards and Technology for their continued support.

This work was sponsored by the Fundamental Aeronautics Program at the NASA Glenn Research Center.

Level of Review: This material has been technically reviewed by technical management.

Available from

NASA Center for Aerospace Information
7115 Standard Drive
Hanover, MD 21076–1320

National Technical Information Service
5285 Port Royal Road
Springfield, VA 22161

Available electronically at http://gltrs.grc.nasa.gov

A Step Towards CO_2-Neutral Aviation

Andreja Brankovic and Robert C. Ryder
Flow Parametrics, LLC
Ivoryton, Connecticut 06442

Robert C. Hendricks
National Aeronautics and Space Administration
Glenn Research Center
Cleveland, Ohio 44135

Marcia L. Huber
National Institute of Standards and Technology
Boulder, Colorado 80305

Summary

An approximation method for evaluation of the caloric equations used in combustion chemistry simulations is described. The method is applied to generate the equations of specific heat, static enthalpy, and Gibb's free energy for fuel mixtures of interest to gas turbine engine manufacturers. Liquid-phase fuel properties are also derived. The fuels investigated include JP–8, synthetic fuel, and two blends of JP–8 and synthetic fuel. The complete set of fuel property equations for both phases are implemented into a computational fluid dynamics (CFD) flow solver database, and multiphase, reacting flow simulations of a well-tested liquid-fueled combustor are performed. The simulations are a first step in understanding combustion system performance and operational issues when using alternate fuels, at practical engine operating conditions.

Introduction

Major issues confronting today's aviation community center on fueling supply and not so much on emissions per se, but on climatic change and the potential for extinction, thus engendering a significant effort to neutralize anthropogenic effects. Realizing that small changes in one area of the planet can make large differences in climatic conditions in other areas (planetary telekinesis[1]), the aviation industry is diligently seeking alternate fueling and combustion methodology to mitigate harmful emissions such as CO_2 and work toward becoming CO_2 neutral. Alternate liquid fuels as derived from coal (CTL) or natural gas (GTL), termed "synfuels," when refined as aviation fuels and combusted, still release significant amounts of CO_2, water, and hydrocarbons, although less than Jet-A. Other plant-derived fuels, termed "biofuels," depend heavily on currently available food crops such as rice, wheat, corn, and soybeans, yet other forms such as switchgrass, algae, halophytes, palm oil, and similar cellulose or oil plant feedstocks, could become effective future fueling feedstock sources. Potentially biofuels could, through carbon trade-off, provide a way for aviation to partially achieve a goal of becoming CO_2 neutral while still using "drop-in" fuels for legacy aircraft. Currently, synfuels and blends are moving through the certification process.

Understanding combustor design and performance issues using alternate fueling is a step toward understanding aviation's impact on climatic change and energy independence. In this report computational combustor performance is baselined to the trapped vortex combustor (TVC) with cavity-only fueling using Jet-A fuel to simulate the experimentally fueled JP8+100 TVC. Prior testing and analysis found JP8+100 and Jet-A to have similar TVC combustion characteristics (ref. 2). This computationally and experimentally established baseline is then compared with that computed using two

[1]Planetary interactions happening in one place, affect other places seemingly without any connection (ref. 1).

other fueling methods, synfuel and JP–8 fuel. Thermophysical properties for these fuels are not yet available from the National Institute of Standards and Technology (NIST), and a method to simulate the needed combustor parameters for these fuels is synthesized and discussed.

The 10-component simulation of synfuel is based on the volume fractions of the major constituents of a synthetic manufactured fuel supplied to the U.S. Air Force Research Laboratory at Wright-Patterson Air Force Base (AFRL/WPAFB). In the lower temperature regime, thermophysical properties of the 10 components are derived from the NIST mixture code SUPERTRAPP (STRAPP) (ref. 3). In the higher temperature regime the properties are derived using a simple specific heat relation $\left(C_p^0/R\right)$ based on the McBride-Gordon NASA thermodynamic code (ref. 4). The JP–8 fuel is simulated in a similar manner using a 12-component mixture. For combustor performance simulations, each multicomponent mixture is treated as a homogeneous fluid.

Based on this chemical mixture information, this work presents CFD-generated cavity-only fueling TVC performance for the following fueling cases:

(1) Liquid JP–8 fuel with gaseous JP–8 fuel real gas properties
(2) Liquid synthetic fuel with gaseous synthetic fuel real gas properties
(3) Liquid JP–8 (50%)/synthetic (50%) fuel blend with associated real gas properties
(4) Liquid JP–8 (70%)/synthetic (30%) fuel blend with associated real gas properties

These fuels and blends were chosen to reflect current and projected fuels used for aviation as well as those fuels available for experimentation including AFRL B52 and C117 flight tests. In interpreting the TVC combustor simulation results, emphasis is placed on combustor quantities of engineering interest, such as spray droplet patterns, combustor flame patterns, and combustor exit plane quantities.

Symbols

A	constant in equation (8), $K^{1/2}$
a_1, a_2, a_3, a_4, a_5, a_6, a_7,	
b_1, b_2	Gordon-McBride coefficients
B	constant in equation (8)
C	carbon number
C_1	constant in equation (9), K
C_2	constant in equation (10)
C/H	carbon-to-hydrogen ratio
$C_p^0(T)/R$	dimensionless specific heat
$G^0(T)/RT$	dimensionless Gibbs free energy
$H^0(T)/RT$	dimensionless enthalpy
H	hydrogen number
MW	molecular weight
R	universal gas constant (i.e., 8.314510 J/(mol-K)
$S^0(T)/R$	dimensionless entropy
T	temperature, K
$U^0(T)/RT$	dimensionless internal energy
ϕ	equivalence ratio

Subscripts:

cav	pertaining to cavity
$C1$=0	calculated with C_1 set to 0
$C2$=0	calculated with C_2 set to 0

overall	pertaining to entire combustor
ref	reference
STRAPP	calculated by STRAPP code

Analysis Methods

Determination of Thermophysical Properties of Advanced, Gaseous Fuels

McBride et al. (ref. 4) established the renowned thermophysical properties code that is the standard for combustion. This code has coefficients for Jet-A, JP–10, and 2000 other species and components that are tabulated in appendix D of NASA/TP—2002–211556 (ref. 4), so $C_p^0(T)/R$ and other caloric properties can readily be determined. Gracia-Salcedo et al. (ref. 5) have shown that 2,2,4-trimethylpentane (isooctane, 224TMP) is a very good caloric simulant for Jet-A; the thermophysical property parameters are available for computations in both McBride et al. (ref. 4) and STRAPP (ref. 3).

Fuel simulations for JP–8 are presented by Heneghan et al. (ref. 6), The JP–8 simulant in the present study comprises 12 components based on those volume fractions. An often-used assumption is that JP8+100 is similar in mixture to the JP–8 simulant. Simulations for synthetic fuels are given by Corporan et al. (ref. 7), Edwards and Maurice (ref. 8), and Edwards et al. (ref. 9). Also, it is assumed that Syntroleum Corporation fuels are similar in composition to the synthetic fuel presented by Corporan et al. (ref. 7); the volume fractions of the major constituents for this fuel are used as the basis for the 10-component simulant of synfuel in the present study. Discussions with Tim Edwards (2006, AFRL/WPAFB) have indicated that Syntroleum fuel could be characterized as n-duodecane (C12).

The NIST computer program NIST4, also called SUPERTRAPP (STRAPP), characterizes fluid mixtures and was developed principally for the hydrocarbon liquid fuels industry. A recent release includes exotetrahydrodicyclopentadiene (JP–10) as well as many of the components found in JP–8 or Syntroleum fuels.

Analytical Procedure

McBride's caloric equations for $C_p^0(T)/R$ form the basis for determining a simplified formulation of caloric properties. McBride provides the following form-similar equations for caloric properties of selected substances as well as the corresponding a_i and b_i coefficients used to compute them (ref. 4):

$$\frac{C_p^0(T)}{R} = \frac{a_1}{T^2} + \frac{a_2}{T} + a_3 + a_4 T + a_5 T^2 + a_6 T^3 + a_7 T^4 \tag{1}$$

$$\frac{H^0(T)}{RT} = a_1 T^2 + \frac{(a_2 \ln T)}{T} + a_3 + \frac{a_4 T}{2} + \frac{a_5 T^2}{3} + \frac{a_6 T^3}{4} + \frac{a_7 T^4}{5} + \frac{b_1}{T} \tag{2}$$

$$S^0(T)/R = \frac{a_1 T^{-2}}{2} - \frac{a_2}{T} + a_3 \ln T + a_4 T + \frac{a_5 T^2}{2} + \frac{a_6 T^3}{3} + \frac{a_7 T^4}{4} + b_2 \tag{3}$$

From the fundamentals of thermodynamics, Gibbs free energy and mixture internal energy are computed, respectively, as

$$\frac{G^0(T)}{RT} = \frac{\left[H^0(T) - TS^0(T)\right]}{RT} = \frac{H^0(T)}{RT} - \frac{S^0(T)}{R} \tag{4}$$

and

$$\frac{U^0(T)}{RT} \approx \frac{H^0(T)}{RT} \tag{5}$$

where

$$\frac{H^0(T)}{RT} = T^{-1}\int\left[\frac{C_p^0(T)}{R}\right]\mathrm{d}T \tag{6}$$

and

$$\frac{S^0(T)}{R} = \int\frac{C_p^0(T)}{RT}\mathrm{d}T \tag{7}$$

In these equations, C_p^0 is the mixture specific heat, H^0 is the mixture static enthalpy, S^0 is the mixture static entropy, G^0 is the mixture Gibbs free energy, and U^0 is the mixture internal energy at zero pressure.

The first set of comparisons were made using McBride's Jet-A coefficients and the $C_p^0(T)/R$ values from the NIST STRAPP code with JP–8 simulant, C12, and 224TMP for the temperature range[2] 300 to 1000 K at a pressure of 0.0001 MPa, shown in figure 1. Although the values are different for a given T, the similarities are striking. Subsequent investigation of the $H^0(T)/RT$ and $S^0(T)/R$ values revealed the same form similarities.

These similarities prompted an investigation for a technique to extrapolate $C_p^0(T)/R$ beyond STRAPP's temperature range to that necessary for combustion computations. A mathematical assessment revealed that McBride's Jet-A $C_p^0(T)/R$ value away from the saturated vapor boundaries could be approximated with the simplified form

$$\frac{C_p^0(T)}{R} = \frac{A}{T^{1/2}} + B \tag{8}$$

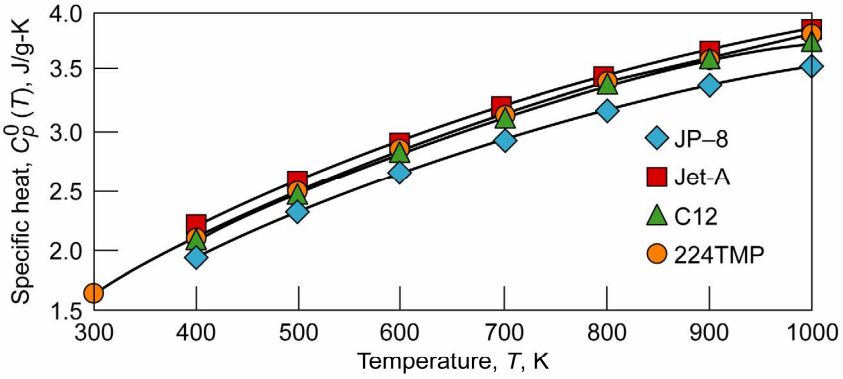

Figure 1.—Similarities of the specific heat values $C_p^0(T)$ for four fuels: two mixtures, JP–8 and Jet-A, and two pure components, n-duodecane (C12) and 2,2,4-trimethylpentane (224TMP). Values are determined from McBride's equations (ref. 4) for Jet-A and STRAPP code (ref. 3) for JP–8, C12, and 224TMP.

[2] The STRAPP code is nominally valid to 600 K.

It then follows that

$$\frac{H^0(T)}{RT} = \frac{2A}{T^{1/2}} + B + \frac{C_1}{T} \tag{9}$$

$$\frac{S^0(T)}{R} = -\frac{2A}{T^{1/2}} + B\ln T + C_2 \tag{10}$$

and Gibb's free energy becomes

$$\frac{G^0(T)}{RT} = \frac{\left[H^0(T) - TS^0(T)\right]}{RT} = \frac{H^0(T)}{RT} - \frac{S^0(T)}{R} \tag{11}$$

In these expressions, the constants C_1 and C_2 are determined by first setting the particular constant (e.g., C_1 for $H^0(T)/RT$) to 0 and determining the matching reference value $H^0(T)_{\text{ref}}/RT_{\text{ref}}$ or $S^0(T)_{\text{ref}}/R$ from those generated by STRAPP or McBride's code depending on the source of the data to be used in the comparison.

$$C_1 = \left\{ T\left[\frac{H^0(T)}{RT}\right]_{\text{STRAPP}} - \left[\frac{H^0(T)}{RT}\right]_{C_1=0} \right\}_{T=T_{\text{ref}}} \tag{12}$$

$$C_2 = \left\{ \left[\frac{S^0(T)}{R}\right]_{\text{STRAPP}} - \left[\frac{S^0(T)}{R}\right]_{C_2=0} \right\}_{T=T_{\text{ref}}} \tag{13}$$

Here T_{ref} was either 300 or 400 K, with the latter providing better overall agreement and usually sufficiently far away from the saturated vapor boundaries.

The liquid-phase properties required for these fuels were determined analytically as well. Of importance to liquid fuel injection, the properties determined included density, specific heat, heat of vaporization, thermal conductivity, and viscosity. These properties were implemented into a CFD flow solver database (from Flow Parametrics, LLC) in order to simulate the droplet dynamics and evaporation characteristics accurately (described in forthcoming sections).

Simplified Form Extrapolations

This simplified form (eq. (8)) permits extrapolation to elevated temperatures, and using the Jet-A $C_p^0(T)/R$ and McBride's equation (1), the constants A and B were determined. The results were compared with the actual $C_p^0(T)/R$ for Jet-A (using McBride's equations) over the range of 300 to 3000 K. The values compared favorably, with a reasonable engineering accuracy of better than 5 percent over the 400 to 3000 K temperature range. However, departures of 20 to 30 percent deviation occur near 300 K, which is close to or on liquid-vapor boundaries. Above 3000 K the deviations continue to fall nearly linearly to 7.5 percent at 6000 K, reflecting the inaccuracies in reproducing the $C_p^0(T)/R$ relative to those calculated using the equations of McBride's code. Better agreement between the extrapolated method and McBride's code predictions is found in the integrated properties, such as $S^0(T)/R$, which for the most part is within about 1 percent, as shown in figure 2. The deviations in $H^0(T)/RT$ depend on at what point the locus changes from negative to positive, where small deviations make large differences. Generally the $H^0(T)/RT$ is within 3 percent. Perhaps a better way to illustrate the deviations would be to add a constant to ensure all values are positive, as is the case with $S^0(T)$/R.

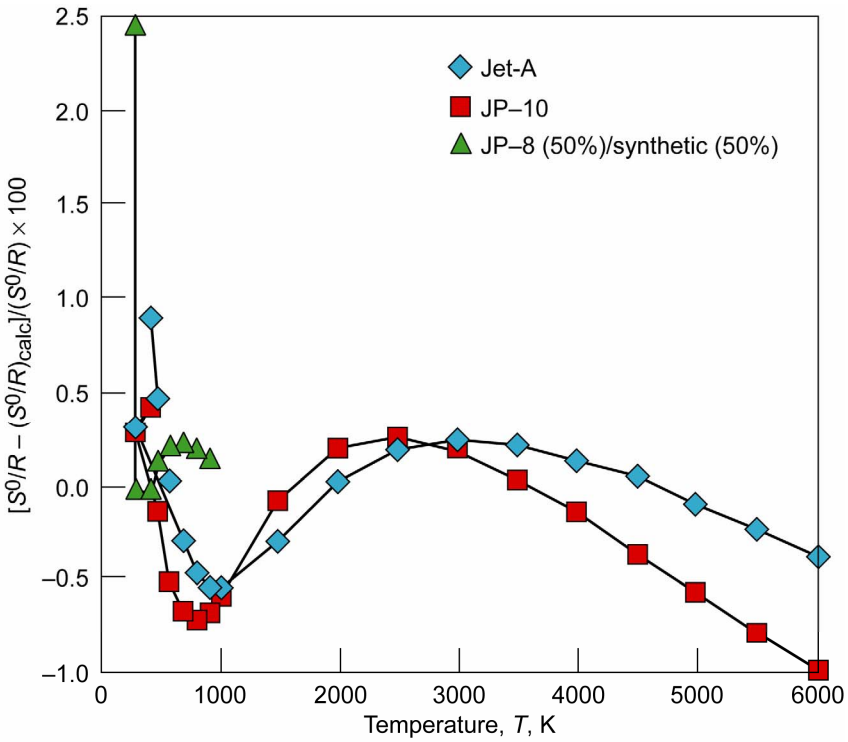

Figure 2.—Deviation between entropy values $S^0(T)/R$ for three jet fuels calculated by simplified extrapolation method and those calculated based on equations from McBride's code.

It was also found that much better overall agreement between McBride and extrapolated values could be generated if the $C_p^0(T)/R$ values were fitted over the range 400 to 3000 K when using data from STRAPP at the lower temperatures. This establishes a methodology to extend $C_p^0(T)/R$, and caloric properties in general, over the range from 300 to 400 K up to 3000 K with reasonable engineering confidence.

STRAPP, Simplified, and McBride Code Comparisons

To illustrate that the simplified form extrapolation technique applies to STRAPP-generated data, McBride's code also has coefficients for the pure-component fluid exotetrahydrodicyclopentadiene (JP–10). Generating $C_p^0(T)/R$, $H^0(T)/RT$, and $S^0(T)/R$ from McBride's method over the range 300 to 3000 K provides the basis for comparison. Using STRAPP input for JP–10, these same values were generated using the simplified extrapolation technique over the range 300 to 1000 K. The values are similar to those found for Jet-A. Using the extrapolation for the range 1000 to 3000 K found similar agreement, thus establishing the technique linking the properties generated by STRAPP with those generated by McBride's code, and it provides reasonable engineering confidence in the caloric computations for mixtures as generated by STRAPP and extrapolated to higher temperatures (fig. 3).

With these comparisons it was then assumed that fluid mixtures characterized by STRAPP in the lower temperature ranges could—through a suitable fit to these data using the simplified method—be extrapolated with reasonable engineering certainty to elevated temperatures in order to characterize combustion. The $C_p^0(T)/R$ and $H^0(T)/RT$ values are important parameters in determining combustion temperature.

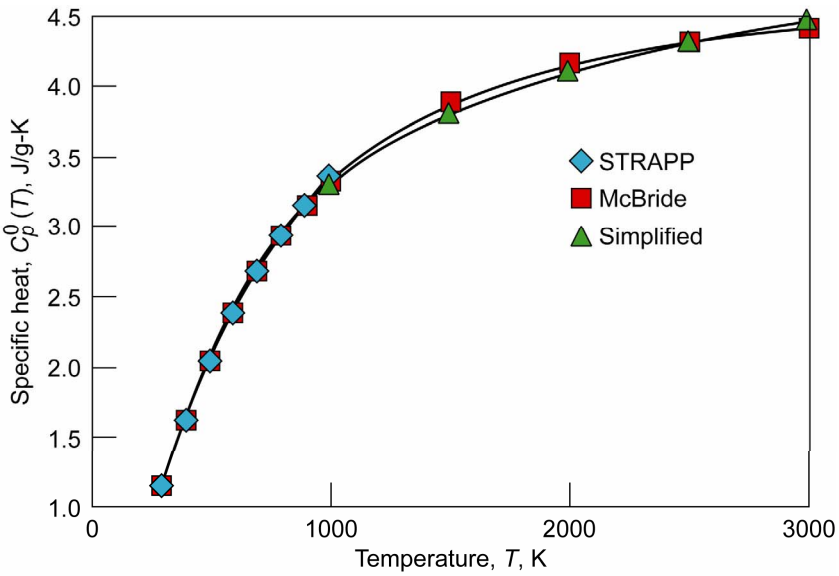

Figure 3.—Comparison between simplified, STRAPP, and McBride extrapolation methods for specific heat values $C_p^0(T)$ for fluid exotetrahydrodicyclopentadiene (JP–10).

The components, volume, and mass fractions used to simulate JP–8 and synthetic fuels are given in tables I and II, respectively. Blended fuel properties were derived using a mole-fraction weighting procedure. The carbon-to-hydrogen ratios (*C*/*H*), molecular weights (*MW*), and simplified extrapolation method constants for each fuel are listed in table III. The *C*/*H* values were determined from the mole fraction product of the *C*/*H* component chemical composition summed over mixture components. In all cases, homogeneous single-component simulations of multicomponent fluid mixtures are used in the combustor simulations, including both liquid and gas phases.

TABLE I.—JP–8 SIMULANT COMPONENTS AND FRACTIONS USED AS INPUT TO STRAPP (REF. 6)

JP–8 component		Mass fraction	Mole fraction	Molecular weight	Mass/weight
2,2,4-trimethylpentane (isooctane)	224TMP	0.0500	0.0640	114.22	0.000437752
Methylcyclohexane	MCC6	.0500	.0745	98.19	.000509217
meta-xylene	MXYL	.0500	.0688	106.17	.000470943
Cyclooctane	CC8	.0500	.0652	112.22	.000445553
n-decane	C10	.1500	.1542	142.28	.001054259
Butylbenzene	C4BNZ	0.0500	0.0545	134.22	0.000372523
1,2,4,5-tetramethylbenzene	1245TMBNZ	.0500	.0652	112.2	.000445633
1,2,3,4-tetrahydronaphthalene (tetralin)	TETRALIN	.0500	.0553	132.2	.000378215
n-dodecane	C12	.2000	.1717	170.34	.001174122
1-methylnaphthalene	1MNAPH	0.0500	0.0514	142.2	0.000351617
n-tetradecane	C14	.1500	.1106	198.39	.000756086
n-hexadecane	C16	.1000	.0646	226.45	.000441599
Mixture (JP–8 simulant)		1.0000	1.0000	[a]146.25 [b]146.25	0.006837519
STRAPP output				147.8	

[a]Value based on mass fraction.
[b]Value based on mole fraction.

TABLE II.—SYNTROLEUM CORPORATION SIMULANT COMPONENTS AND FRACTIONS USED AS INPUT TO STRAPP (REF. 7).

Syntroleum component		Mass fraction	Mole fraction	Molecular weight	Mass/weight
n-octane	C8	0.0430	0.0570	114.22	0.000376466
n-nonane	C9	.1000	.1181	128.26	.000779666
n-decane	C10	.1870	.1990	142.28	.00131431
n-undecane	C11	.1900	.1841	156.31	.001215533
n-dodecane	C12	.1320	.1174	170.34	.000774921
n-tridecane	C13	0.0930	0.0764	184.36	0.000504448
n-tetracecane	C14	.0740	.0565	198.39	.000373003
n-pentadecane	C15	.0270	.0192	212.42	.000127107
3-methyloctane	3MO	.0720	.0850	128.26	.00056136
2-methylnonane	2MN	.0820	.0873	142.29	.000576288
Mixture (Syntroleum simulant)		1.0000	1.0000	[a]151.44 [b]151.44	0.006603101
STRAPP output				151.4	

[a]Value based on mass fraction.
[b]Value based on mole fraction.

TABLE III.—CARBON-TO-HYDROGEN RATIOS (*C*/*H*), MOLECULAR WEIGHTS (*MW*), AND CONSTANTS FOR EQUATIONS (8) THROUGH (10) USED IN SIMPLIFIED EXTRAPOLATION METHOD FOR INVESTIGATED FUELS

Fuel	Input for simplified extrapolation method					
	C/*H*	*MW*	*A*	*B*	C_1	C_2
JP–8	10.605/20.15	147.83	–1542.6	110.9	–314.83	–746.54
JP–8 (70%)/synthetic (30%)	10.629/21.72	148.94	–1582.4	113.9	–2321.47	–763.57
JP–8 (50%)/synthetic (50%)	10.620/21.09	149.60	–1607.3	115.8	–3673.2	–775.93
Synthetic	10.653/23.306	151.40	–1671.8	120.68	–6983.8	–808.36

Liquid-phase fuel properties are required to describe the initial injection of liquid-fuel spray droplets into the combustor through orifice injectors. These were derived using a mole-fraction weighting procedure. Key liquid property values are indicated in table IV, including liquid molecular weight, boiling point at 0.1 MPa, density, and latent heat of vaporization. Additional property values required for accurate spray droplet dynamics and evaporation rates include specific heat, viscosity, and thermal conductivity, which were also determined as part of this effort.

TABLE IV.—LIQUID-PHASE FUEL PROPERTIES FOR INVESTIGATED FUELS

Fuel	Liquid-phase fuel properties[a]				
	Molecular weight	Boiling point at 0.1 MPa, K	Density at 298 K, kg/m^3	Density at boiling point,[b] kg/m^3	Latent heat, kJ/kg
JP–8	147.83	436.3	800.7	681.7	255.0
JP–8 (70%)/synthetic (30%)	148.94	439.6	783.6	660.5	287.0
JP–8 (50%)/synthetic (50%)	149.6	441.7	772.8	647.0	296.0
Synthetic	151.4	447.2	747.0	614.6	290.0

[a]Isothermal flash properties (from NIST, ref. 3).
[b]One or two components may be in solid phase.

We have now shown that

(1) The simplified method is a good representation of the McBride $C_p^0(T)/R$ values to within reasonable engineering certainty.

(2) There is good agreement between the NIST code STRAPP and the McBride values for $C_p^0(T)/R$ over the range 400 to 1000 K, recognizing that 600 to 1000 K is an overextension of STRAPP.

(3) The simplified method is a good representation of the STRAPP $C_p^0(T)/R$ away from the saturation vapor boundary.

(4) Therefore, the simplified method with coefficients (A, B,C1, and C2) determined using the STRAPP values (or McBride values where applicable) is a valid representation for mixtures and components of the NIST code over the range 400 to 3000 K.

(5) Fluid properties required in this analysis, near or on the saturation liquid or vapor boundaries, can be determined from STRAPP.

This establishes the necessary thermophysical properties required by the flow solver to determine the combustion characteristics. We now turn to the TVC combustor fueling computations, comparisons, results, and discussions.

Trapped Vortex Combustor Experimental Rig

The trapped vortex combustor (TVC) sector rig at the AFRL/WPAFB is used as the experimental basis. It is a combustor geometry for which there exists a wealth of validation data including, for example, wall pressures, emissions, and high-frame-rate video for flame structure. The inlet diffuser and combustor geometries are accurately described with computer-aided design (CAD), with known coolant flows and spray droplet characterizations. The TVC operates stably over a wide range of equivalence ratios and pressures and has been useful in studies of altitude restart and lean blow out (LBO) (refs. 2 and 10). A schematic of the test rig is shown in figure 4(a), which illustrates the airflow and fuel injection sites as well as the general flow patterns expected in the combustor.

Provision for addition of water mist for pollutant emission reduction studies is also indicated. A photograph of the combustor hardware is shown in figure 4(b), with the sidewall removed for optical access. Components of the rig include the tripass diffuser, combustor bulkhead, heat shield, and combustor duct that exhausts to a vent. Combustor walls are cooled through effusion holes along the entire interior wall and film cooling through slots along the combustor upper and lower walls.

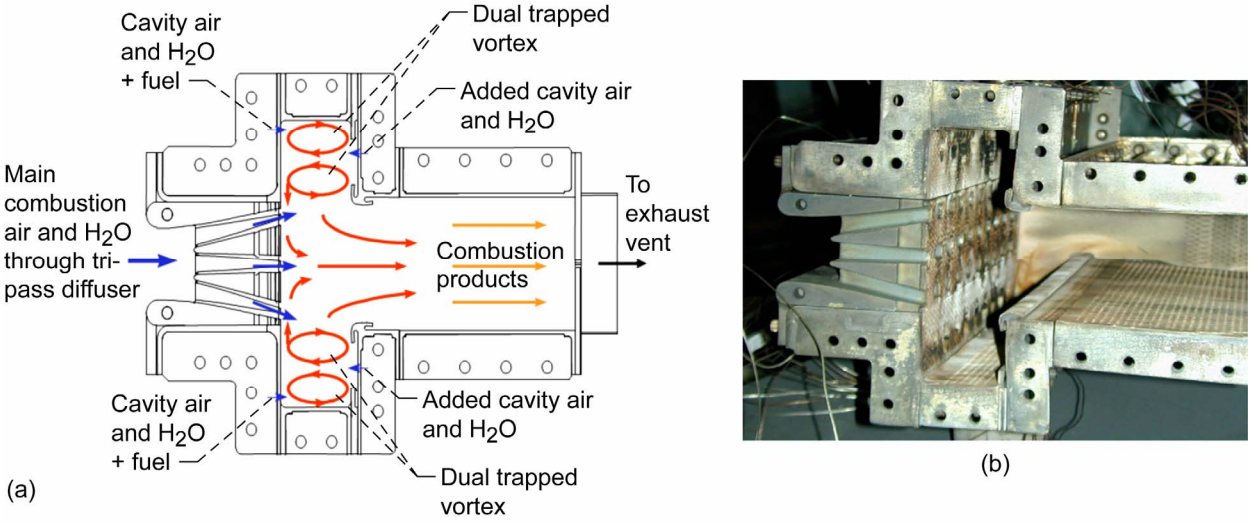

Figure 4.—(a) Trapped vortex combustor (TVC). Arrows indicate major flow components. Liquid fuel is injected into TVC cavity and also directly into main combustor through orifices in diffuser. For present study, cavity-only fuel injectors are utilized without water injection. (b) Test rig hardware for TVC, with near sidewall removed for optical access. Photograph shows 10 fuel injector modules in spanwise direction.

Engine compressor exit air is emulated by a plenum and is connected to the TVC combustor through a tripass diffuser. This diffuser configuration splits the flow evenly, with the upper and lower diffuser flow paths providing high-speed shear layers that drive the cavity flows and entrain products of combustion into the main flow.

The center diffuser flow path provides a high-speed jet that interacts with the outer diffuser flows and further mixes the products as the flow approaches the combustor exit. The result is a stable combustion process with high efficiency, within a compact configuration. The TVC combustor is fueled in two different ways. Liquid fuel is injected through simple orifice injectors into the main diffuser flow paths, with the high-speed crossflow atomizing the liquid fuel jet into a fine mist. Independently, liquid fuel is injected into the TVC cavities through simple orifice injectors. The cavity spray droplets are injected into a hot, reacting flow environment and evaporate rapidly. Using this experimental rig, and through a combination of cavity-only, cavity and main, and main-only fueling schemes, different operating conditions can be produced in the rig, allowing for investigation of a wide variety of flow phenomena in the experiment.

The effect of the spray droplet injection conditions on the combustor flow field and combustor exit pattern factor has been investigated previously (ref. 10). During that effort, the initial droplet size distributions were determined for the engine operating conditions used in this investigation. For the main injector and for a nominal plenum pressure of 50 psia (344.6 kPa), the Rosin-Rammler droplet size distribution was $R_{32,10}$ = 3 μm, $R_{32,50}$ = 6 μm, and $R_{32,90}$ = 12 μm. For the cavity injector, the Rosin-Rammler droplet size distribution was $R_{32,10}$ = 5 μm, $R_{32,50}$ = 8 μm, and $R_{32,90}$ = 10 μm. The effects of water misting and water injection through the orifice injectors were also studied (ref. 11), showing computationally the potential benefits of water addition to reduction of NOx at the combustor exit.

Both of those parametric studies above showed the significant variation in combustor exit parameters (average temperature, combustion efficiency, and flame structure and pattern factor) due to even small upstream differences in liquid fuel droplet size and fuel water vapor content.

In the present parametric study, therefore, the droplet size distribution and overall cavity-based equivalence ratio are held constant; only the fuels are varied to isolate the effects that differences in their liquid and gas properties have on combustor characteristics. The cavity equivalence ratio ϕ_{cav} = 2.2 for each case, while the overall equivalence ratio (entire combustor including all combustion, driving, and cooling flows) $\phi_{overall}$ = 0.53.

Computational Fluid Dynamics Simulations Using Alternate Fuels

To characterize the performance of the various fuels in the TVC test rig, a suite of computational CFD simulations are performed. The four fuels investigated include JP–8, synthetic, and blended fuels consisting of JP–8 (50%)/synthetic (50%) and JP–8 (70%)/synthetic (30%) by volume. All corresponding liquid and gas properties for each fuel have been derived based on data in tables III and IV and installed in the flow solver property database. Combustion chemistry is modeled using the three-step reduced chemistry model of Molnar and Marek (ref. 12), which consists of a fuel breakup and oxidation equation into CO and H_2O (Step 1), oxidation of CO into CO_2 (Step 2), and dissociation of N_2 and O_2 into NOx (Step 3). Previous validation studies (refs. 2, 10, and 11) provide useful information on injection conditions for the liquid fuel, including droplet diameter distributions, velocities, and spray cone angles.

The test rig geometry is accurately represented in the form of a CAD solid model. Using the CAD model, all boundary conditions are tagged, including all major inflows, secondary flows, and film cooling slots. Following this, the volume is discretized using an unstructured mesh generator. The model is exported, and the domain is decomposed and load balanced for running on parallel networked computers for rapid turnaround time. Results are postprocessed graphically and quantitatively using a mass-averaging algorithm.

Results of Flow Simulations

The basis for comparison of the combustor simulations is inspection of the computed flame structure at the TVC midplane and computed mass-averaged quantities at the combustor exit. Comparison of the flame structure for the four different fuels is shown in figure 5. The contours shown are each taken at the combustor midplane, using the same temperature scale, allowing direct comparison.

The flow structure is similar, nearly identical, for each fuel. Upon inspection of the fuel properties, both liquid and gas, this is not unexpected. The flow structure similarity suggests that droplet evaporation and dynamics patterns are nearly identical, resulting in the similar burning patterns. Each of the combustor simulations exhibits a centrally peaked temperature profile at the flow exit. The effects of multicomponent spray modeling are yet to be determined.

Carbon monoxide generation and flow pattern is shown in figure 6 for the four cases. Rapid formation of CO in the TVC cavities is observed for each case. As the cavity flow is entrained by the diffuser flow and further heated within the combustor, the CO oxidizes into CO_2; this oxidation process is observed in the CO_2 contours shown in figure 7, again for each of the four fuels.

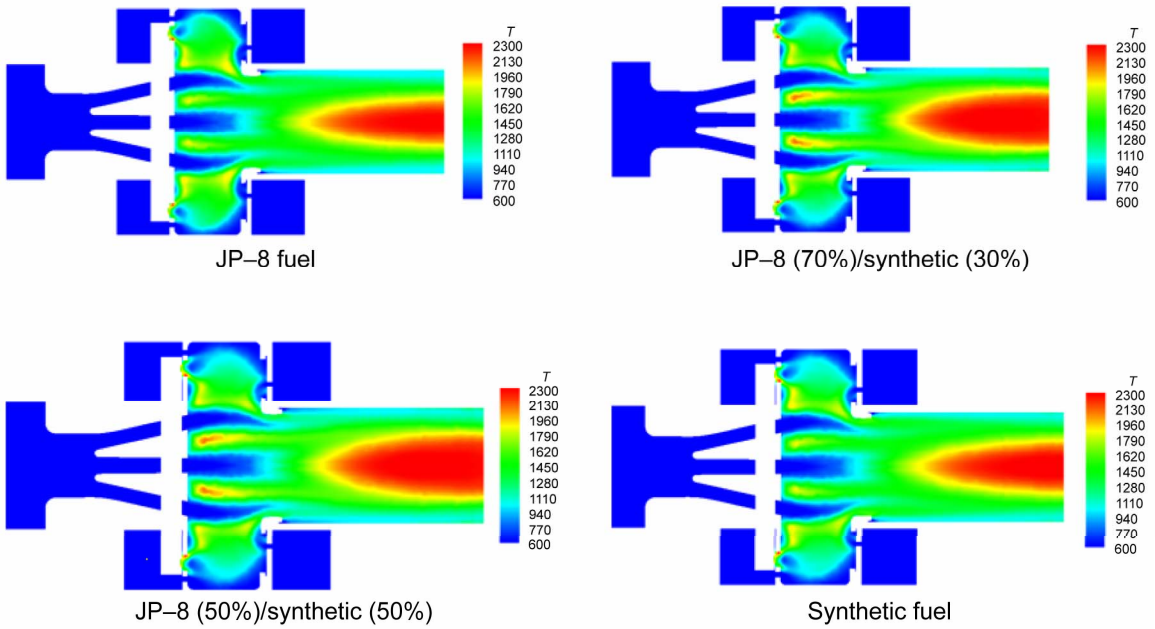

Figure 5.—Combustor midplane contours of static temperature *T* (in Kelvins) for labeled fuels.

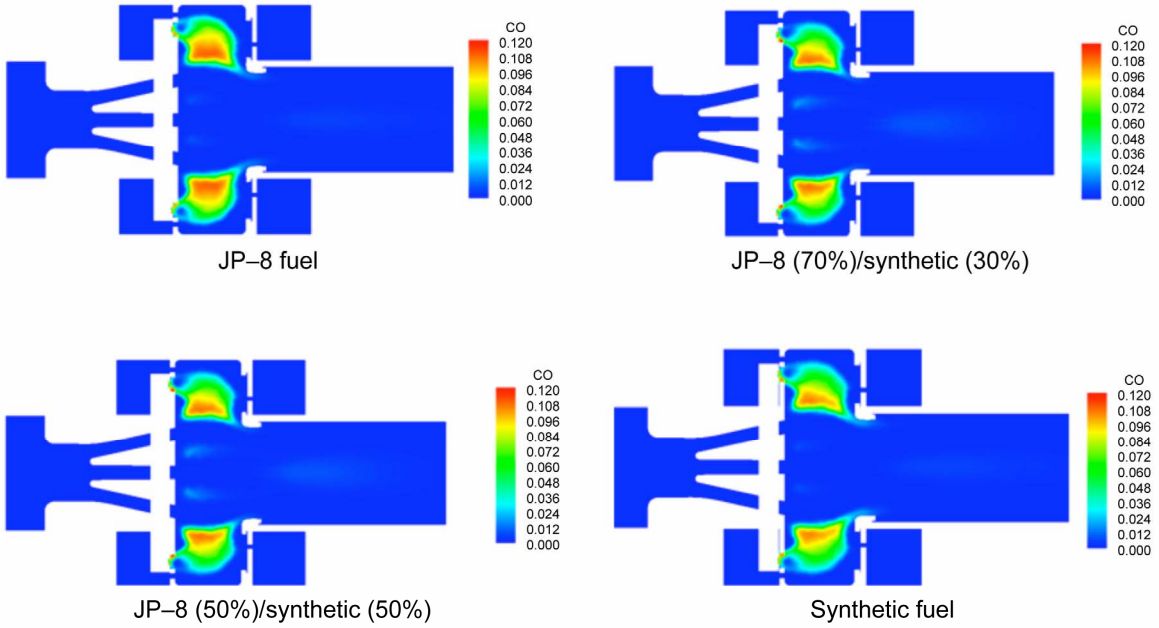

Figure 6.—Combustor midplane contours of carbon monoxide (CO) mass fraction for labeled fuels. Strong peaks occur within high residence time cavities; with increased time and temperature, the majority of CO oxidizes to CO_2 as flow reaches combustor exit plane.

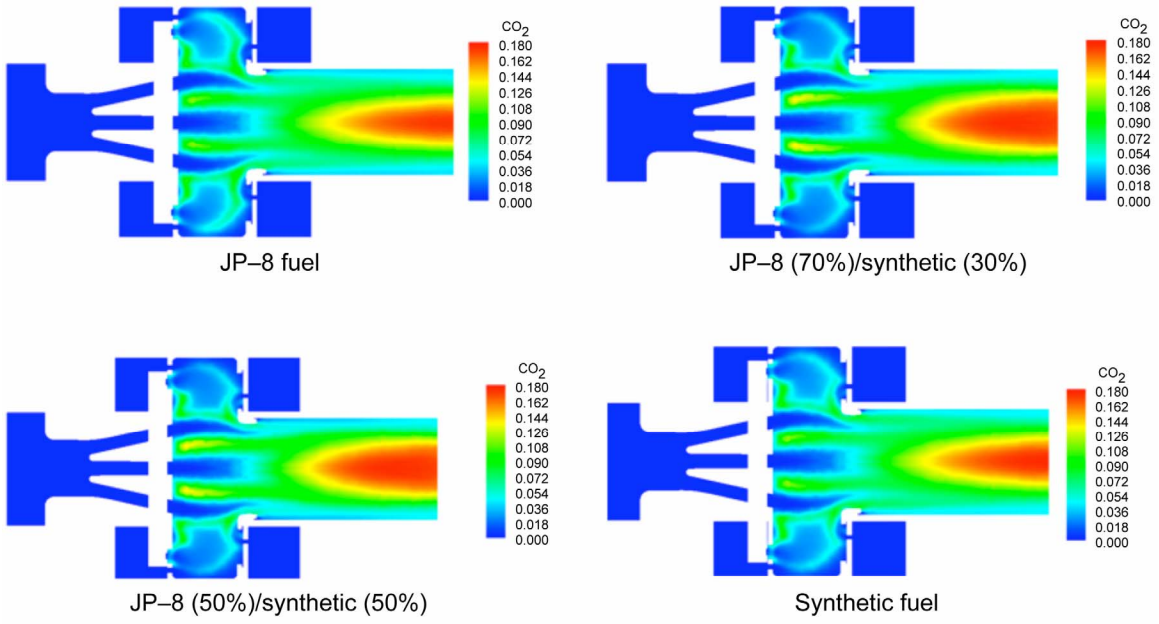

Figure 7.—Combustor midplane contours of carbon dioxide (CO_2) mass fraction for labeled fuels. A characteristic CO_2 formation pattern is observed in each case, with strong centrally oriented peaks occuring as flow exits combustor.

Combustor exit quantities are provided in table V. The values were obtained by mass averaging the computed flow field at the combustor exit. Temperatures vary by about 24 K (or about 1.5 percent maximum to minimum) at that location. Thus, despite strong similarities in computed flow structure, this temperature difference produced by these fuels is potentially enough to require alterations in the cooling scheme for the turbine first vane in a practical application. An inspection of the tabulated values shows that the highest exit temperatures correspond to the least amount of unburned fuel at the exit. Likewise, lowest exit temperatures correspond to greatest amounts of unburned fuel. The minor differences in fueling that occur upstream in the cavities and combustor are apparently enough to cause significant differences in the engineering quantities sampled at the combustor exit.

TABLE V.—COMPUTED COMBUSTOR EXHAUST PLANE QUANTITIES OF INVESTIGATED FUELS

Fuel	Mass-averaged combustor exit quantities			
	Temperature, K	CO mass fraction	CO_2 mass fraction	Unburned fuel mass fraction
JP–8	1600.0	0.00031	0.094	0.00049
JP–8 (70%)/synthetic (30%)	1622.9	0.00030	0.097	0.00042
JP–8 (50%)/synthetic (50%)	1624.1	0.00029	0.097	0.00042
Synthetic	1603.1	0.00039	0.096	0.00057

Increases in CO and unburned hydrocarbon mass fractions, indicated in table V, become a relative measure of how these fuels respond within the tripass TVC combustor. Computations show that synfuel droplet sprays have longer residence times within the combustor relative to JP–8 or blended fuels, although Moses (ref. 13) shows “no effect” of CO or other emissions of synfuel relative to Jet-A; experimental TVC data are needed to resolve this issue. Emission signatures are important especially to the military cross-platform common fuels initiative.

In addition to these comparisons, the complex flow structure is studied in a three-dimensional sense using animations. These flow animations can be viewed in the PDF file of this document found online at http://gltrs.grc.nasa.gov. A series of still images taken from an animation of the flow is shown in figure 8; the animations become active by clicking on each image in the figure in the online report found at http://gltrs.grc.nasa.gov. In each, the TVC combustor geometry is shown translucently to view the inside of the flow. Particle paths are seeded at representative locations, such as upstream in the diffuser legs, inside the plenums with driving airflow, and inside the cavity itself. The particle paths trace out the gas phase flow and are colored by local gas phase static temperature. Numerous vortices are observed inside the driven cavity, and that flow is entrained by the diffuser leg flow. Some of the heated products of combustion are trapped along the inner combustor wall, between the center and outer diffuser legs. This serves as flameholder acting upon the center flow. Comparison of these results with high-frame-rate videos and long-time-averaged still photos of the flow show good consistency in flame shape (ref. 11).

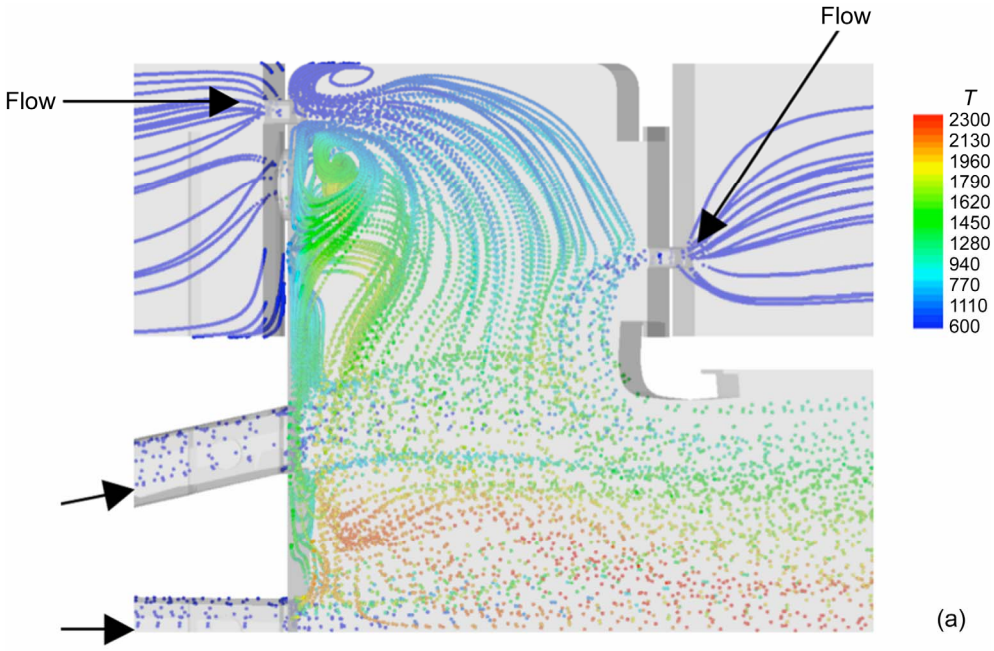

Click here to play movie

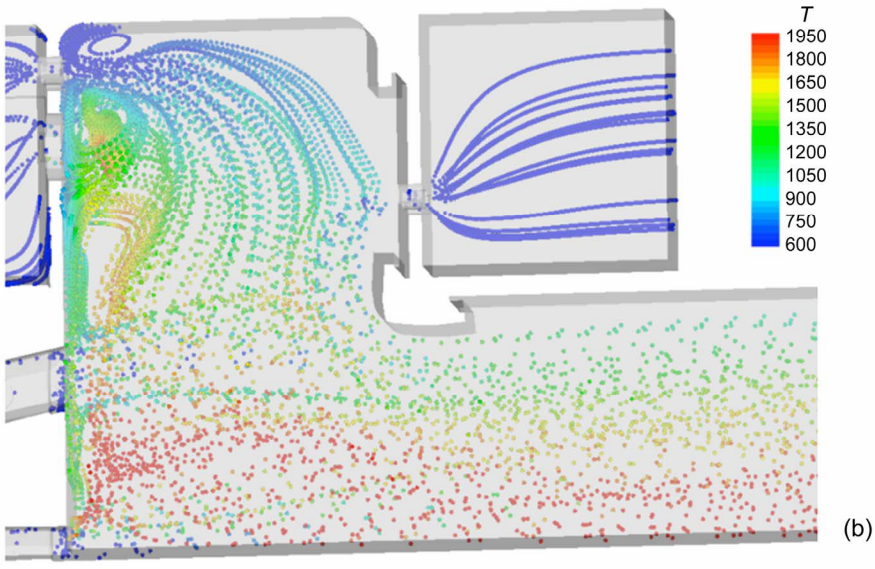

Click here to play movie

Figure 8.—Frames from animation of thermal flow fields simulated by computational fluid dynamics. Solid particles color coded by local gas temperature (temperature *T* is in Kelvins) are used to visualize flow in the trapped vortex combustor (TVC) cavity and combustor duct. (a) Isometric, mainly lateral view, with emphasis on the mixing region between diffuser, cavity and combustor flow. Arrows indicate flow directions. (b) Similar to (a) with more downstream mixing shown.

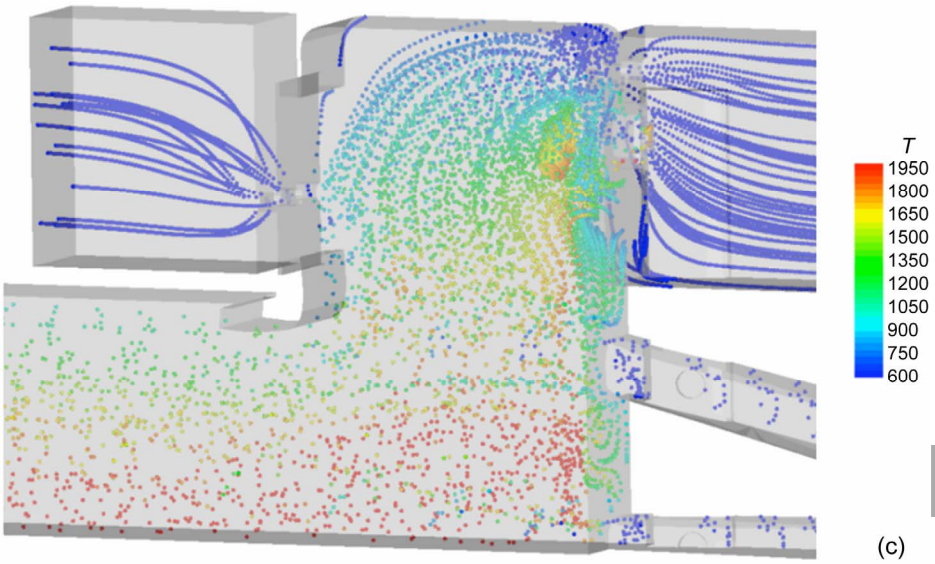

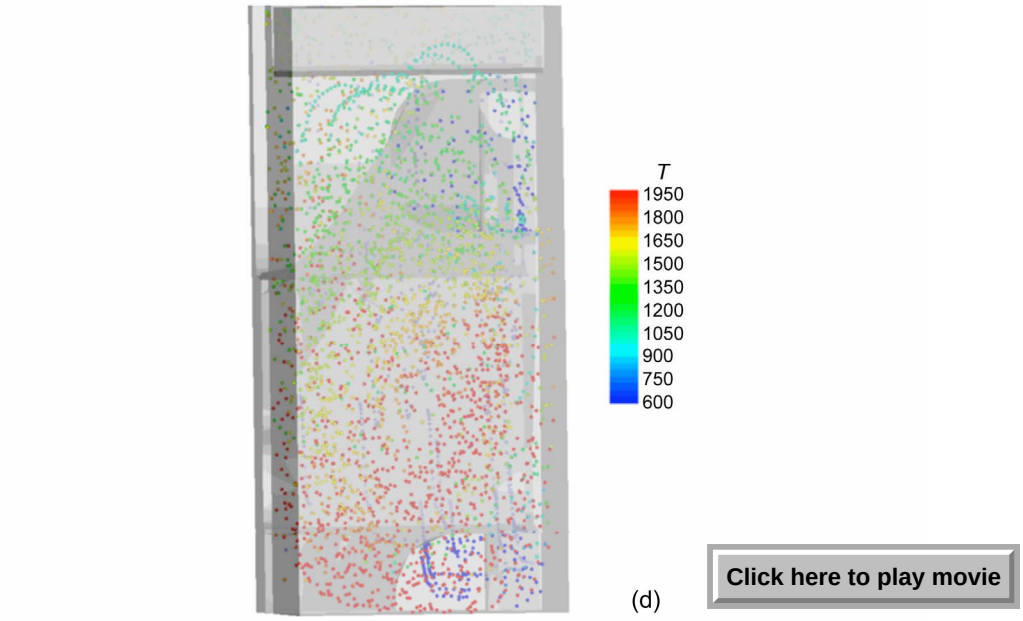

Figure 8.—Concluded. (c) Reversed isometric view, showing more of the combustor flow downstream. (d) Aft-looking forward view towards orifice fuel injectors, showing some overall cross-sectional mixing pattern as it expands in lengthwise direction.

Conclusion

The simplified form of the gas phase caloric equations generated using the NIST STRAPP code, the NASA McBride code, and a systematic curve-fitting methodology, work well within an established computational fluid dynamics (CFD) flow solver. Upon further benchmarking, the actual code speed-up for combustion chemistry CFD cases in practical geometries will be quantified. Computed flow structure for the four fuels studied—JP–8, synthetic fuel, and two blends of these—using a trapped vortex combustor experimental rig as a test case, show strong similarities. This is true for the temperature as well as the CO and CO_2 mass fraction contours. Inspection of the mass-averaged combustor exit quantities, however, indicates that temperature differences may be sufficient to require reconsideration of turbine fueling schemes. Experimental validation studies using these fuels, over a range of operating conditions, are expected.

References

1. Flannery, Tim F.: The Weather Makers: How Man Is Changing the Climate and What It Means for Life on Earth. Atlantic Monthly Press, New York, NY, 2005.
2. Hendricks, R.C.; Shouse, D.T.; Roquemore, W.M.; Burrus, D.L.; Duncan, B.S.; Ryder, R.C.; Brankovic, A.; Liu, N.-S.; Gallagher, J.R.; and Hendricks, J.A.: Experimental and Computational Study of Trapped Vortex Combustor Sector Rig With High-Speed Diffuser Flow. Int. J. Rotating Machinery, vol. 7, no. 6, 2001, pp. 375–385.
3. Huber, M.L.: NIST Thermophysical Properties of Hydrocarbon Mixtures Database: Version 3.2. NIST Standard Reference Database 4, National Institute of Standards and Technology, 2007.
4. McBride, Bonnie J.; Zehe, Michael J.; and Gordon, Sanford: NASA Glenn Coefficients for Calculating Thermodynamic Properties of Individual Species. NASA/TP—2002-211556, 2002.
5. Gracia-Salcedo, Carmen M.; Brabbs, Theodore A.; and McBride, Bonnie J.: Experimental Verification of the Thermodynamic Properties for a Jet-A Fuel. NASA TM–101475 (AVSCOM Technical Report 88–C–014), 1988.
6. Heneghan, Shawn P.; Locklear, Stacy L.; Geiger, David L.; Anderson, Steven D.; and Schulz, William D.: Static Tests of Jet Fuel Thermal and Oxidative Stability. J. Propul. P., vol. 9, no. 1, 1993, pp. 5–9.
7. Corporan, E.; DeWitt M.J.; Belovich, V.; Pawlik, R.; Lynch, A.C.; Gord, J.R.; and Meyer, T.R.: Emissions Characteristics of a Turbine Engine and Research Combustor Burning a Fischer-Tropsch Jet Fuel. Energy and Fuels, vol. 21, no. 5, 2007, pp. 2615–2626.
8. Edwards, Tim; and Maurice, Lourdes Q.: Surrogate Mixtures to Represent Complex Aviation and Rocket Fuels. J. Propul. P., vol. 17, no. 2, 2001, pp. 461–466.
9. Edwards, T.; Minus, D.; Harrison, W.; and Corporan, E.: Fischer-Tropsch Jet Fuels—Characterization for Advanced Aerospace Applications. AIAA–2004–3885, 2004.
10. Hendricks, R.C.; Ryder, R.C.; Brankovic, A.; Shouse, D.T.; Roquemore, W.M.; and Liu, N.-S.: Computational Parametric Study of Fuel Distribution in an Experimental Trapped Vortex Combustor Sector Rig. ASME GT2004–53225, 2004.
11. Brankovic, A.; Ryder, R.C.; Hendricks, R.C.; Liu, Nan-Suey; Shouse, D.T.; and Roquemore, W.M.: Emissions Prediction and Measurement for Liquid Fueled TVC Combustor With and Without Water Injection. AIAA–2005–0215, 2005.
12. Molnar, Melissa; and Marek, C. John: Reduced Equations for Calculating the Combustion Rates of Jet-A and Methane Fuel. NASA/TM—2003-212702, 2003.
13. Moses, C.: Sasol Synthetic Jet Fuel Program. JP–900 Jet Fuel Summit Meeting, Pennsylvania State University, State College, PA, June 2006. (Available from H.H. Schobert, Editor-Facilitator, schobert@ems.psu.edu or http://www.matse.psu.edu/fac/profiles/shobert.htm.)

REPORT DOCUMENTATION PAGE	Form Approved OMB No. 0704-0188

1. REPORT DATE *(DD-MM-YYYY)*	2. REPORT TYPE	3. DATES COVERED *(From - To)*
01-08-2008	Technical Memorandum	

4. TITLE AND SUBTITLE
A Step Towards CO_2-Neutral Aviation

5a. CONTRACT NUMBER

5b. GRANT NUMBER

5c. PROGRAM ELEMENT NUMBER

6. AUTHOR(S)
Brankovic, Andreja; Ryder, Robert, C.; Hendricks, Robert, C.; Huber, Marcia, L.

5d. PROJECT NUMBER

5e. TASK NUMBER

5f. WORK UNIT NUMBER
WBS 561581.02.08.03.16.03

7. PERFORMING ORGANIZATION NAME(S) AND ADDRESS(ES)
National Aeronautics and Space Administration
John H. Glenn Research Center at Lewis Field
Cleveland, Ohio 44135-3191

8. PERFORMING ORGANIZATION REPORT NUMBER
E-16128-1

9. SPONSORING/MONITORING AGENCY NAME(S) AND ADDRESS(ES)
National Aeronautics and Space Administration
Washington, DC 20546-0001

10. SPONSORING/MONITORS ACRONYM(S)
NASA

11. SPONSORING/MONITORING REPORT NUMBER
NASA/TM-2008-214998

12. DISTRIBUTION/AVAILABILITY STATEMENT
Unclassified-Unlimited
Subject Categories: 34, 01, 05, and 59
Available electronically at http://gltrs.grc.nasa.gov
This publication is available from the NASA Center for AeroSpace Information, 301-621-0390

13. SUPPLEMENTARY NOTES
Videos of the animations for figure 8 can be viewed in the PDF file of this report at the Web site http://gltrs.grc.nasa.gov.

14. ABSTRACT
An approximation method for evaluation of the caloric equations used in combustion chemistry simulations is described. The method is applied to generate the equations of specific heat, static enthalpy, and Gibb's free energy for fuel mixtures of interest to gas turbine engine manufacturers. Liquid-phase fuel properties are also derived. The fuels investigated include JP-8, synthetic fuel, and two blends of JP-8 and synthetic fuel. The complete set of fuel property equations for both phases are implemented into a computational fluid dynamics (CFD) flow solver database, and multiphase, reacting flow simulations of a well-tested liquid-fueled combustor are performed. The simulations are a first step in understanding combustion system performance and operational issues when using alternate fuels, at practical engine operating conditions.

15. SUBJECT TERMS
Avation; Emissions; Combustor fundamentals; CFD

16. SECURITY CLASSIFICATION OF:			17. LIMITATION OF ABSTRACT	18. NUMBER OF PAGES	19a. NAME OF RESPONSIBLE PERSON
a. REPORT	b. ABSTRACT	c. THIS PAGE			STI Help Desk (email:help@sti.nasa.gov)
U	U	U	UU	22	19b. TELEPHONE NUMBER *(include area code)* 301-621-0390